Seismic Amplification of Soil Ground with Spatially Varying Shear Wave Velocity Using 2D Spectral Element Method

Duruo Huang, Gang Wang, Chunyang Du & Feng Jin

Taylor & Francis
Taylor & Francis Group

Check for updates

Seismic Amplification of Soil Ground with Spatially Varying Shear Wave Velocity Using 2D Spectral Element Method

Duruo Huang[a], Gang Wang[b], Chunyang Du[b], and Feng Jin[a]

[a]Department of Hydraulic Engineering, Tsinghua University, Beijing, China; [b]Department of Civil and Environmental Engineering, The Hong Kong University of Science and Technology, Hong Kong SAR

ABSTRACT

Spatial variability of soils can have a profound effect on seismic site amplification, which cannot be reasonably captured using conventional one-dimensional analyses. In this study, the shear-wave velocity of soils is modelled as a 2D spatially correlated random field. Extensive simulations are conducted to quantify the influence of spatial variability of soils on site amplification using 2D Spectral Element Method. Key influential factors include variation and spatial correlation of shear wave velocity in both horizontal and vertical directions. Numerical simulations show that site amplification at resonance frequencies is subdued, and its variation depends on these influential factors. Spatial correlations of site amplification are also investigated, showing that the correlation range of site amplification is frequency dependent. The correlation range is much longer at low frequencies than that at high frequencies. The analyses imply that length scales of both soil heterogeneity and wavelength should be considered simultaneously when quantifying the spatial variability of ground motion amplification.

1. Introduction

Amplification of propagated seismic waves in soils has often been observed as one of the major causes of intensive damage in past earthquakes [e.g. Kawase, 1996; Flores-Estrella *et al.*, 2007; Bradley *et al.*, 2018]. Previously, seismic site response analysis has often been conducted using one-dimensional models. A few analytical investigations have been conducted for layered inhomogeneous soil with modulus varying with depth [Gazetas, 1982; Towhata, 1996; Afra and Pecker, 2002; Travasarou and Gazetas, 2004; Mylonakis *et al.*, 2011; Rovithis *et al.*, 2011; Zhang *et al.*, 2017, 2019]. Numerical models, such as the equivalent linear (EQL) method and its variants, or a fully nonlinear method, are often used in 1D site response analyses [Schnabel *et al.*, 1972; Idriss and Sun, 1992; Hashash and Park, 2002; Park and Hashash, 2004; Rathje *et al.*, 2010; Kaklamanos *et al.*, 2013, 2015; Huang *et al.*, 2018]. However, all above analyses assume soils are layered and extend infinitely in the horizontal direction. The 1D model has been reported to be insufficient in estimating ground responses of adjacent soil columns with different material properties [Pehlivan *et al.*, 2012]. Seismic scattering effect, that is, seismic waves are modified by

heterogeneities, cannot be accounted for in 1D ground response analyses. Yet, 2D and 3D analyses are rarely conducted due to their complexity.

Due to different depositional history, soil properties vary from one location to another even within relatively homogenous deposit. Field investigation of surficial geologic sediments in North California shows that shear wave velocity varies with coefficient of variation (COV) 0.15–0.2 within each geologic unit [Holzer et al., 2005]. Only a few site investigations have been conducted to quantify the spatial correlation structure of soil properties at a site-specific scale. In general, the horizontal correlation is stronger than the vertical due to horizontal layering of sediments. Geostatistical studies show that horizontal correlations of soil properties are at the scale of meters to tens of meters while the vertical correlations are on the order of centimeters to meters [Elkateb et al., 2003; Thompson et al., 2009]. For undrained shear strength in clays, Soulie et al. [1990] found the horizontal correlation range of 30 m and a vertical range of 3 m. DeGroot [1996] analyzed the spatial variability of in-situ soil properties and found the correlation ranges are 15–30 m in the horizontal direction and 0.5–3 m in the vertical direction. Recent numerical examples clearly demonstrated that spatial variability of soil strength has significant effects on bearing capacity of the ground [Wu et al., 2019].

Soil variability and its spatial distribution in both horizontal and vertical directions can have a profound effect on site amplification. Therefore, modeling the soils as spatially correlated random fields can significantly improve prediction of the ground response against recorded field data [Thompson et al., 2010]. In this study, extensive simulations are conducted to quantify the influence of spatial variability in soil profiles on site amplification through 2D numerical analyses. The shear wave velocity distribution within the site is modelled by a 2D spatially correlated random field. Parametric studies are carried out by varying key influential factors, including variation of shear-wave velocity and its horizontal/vertical spatial correlations. Based on numerical studies, the research provides empirical relation between variability in seismic ground amplification and that in heterogeneous soil medium, which would be useful to improve scientific understanding of propagation of variability in seismic ground response analyses.

2. Spectral Element Modelling of Spatially Varying Ground

2.1. *Modeling Spatially Correlated Shear Wave Velocity*

In this study, the shear wave velocity of the site is modelled as a spatially correlated random field. At a given location, the shear wave velocity is assumed to be log-normally distributed with a specified mean V_s and variance. Spatially, the values of shear wave velocity are correlated. The distance at which the correlation diminishes is called the range. The variance and the range characterizes the heterogeneity of the shear wave velocity as a spatially distributed random variable.

In this study, the semivariogram analysis is adopted to model the shear wave velocity of soils as spatially correlated random field [Goovaerts, 1997]. Semivariogram analysis has been extensively used as a geostatistical tool for modeling regionalized variables, such as spatially distributed ground motions and ground-motion intensity measures [Park and Hashash, 2004; Huang and Wang, 2015a, 2015b; Wang and Du, 2013; Du and Wang, 2014]. The empirical semivariogram, $\gamma(h)$, can be estimated using the following equation:

$$\gamma(h) = \frac{1}{2N(h)} \sum_{1}^{N(h)} [V_s(x+h) - V_s(x)]^2 \qquad (1)$$

where $V_s(x)$ is shear wave velocity at location x, h denotes the separation distance, $N(h)$ is the number of data pairs separated at a distance h. The semivariogram can be fitted using an exponential model [Wang and Du, 2013; Du and Wang, 2014; Huang and Wang, 2015a, 2015b], with the following functional form:

$$\tilde{\gamma}(h) = a\left[1 - exp\left(-\frac{3h}{R}\right)\right] \qquad (2)$$

where a and R denote sill and correlation range of a semivariogram, respectively. The exponential model specifies that 95% of the spatial correlation vanishes beyond the range R. Accordingly, the spatial correlation function $\rho(h)$ can be written as:

$$\rho(h) = exp\left(-\frac{3h}{R}\right) \qquad (3)$$

Assuming the shear-wave velocity follows a lognormal distribution, the 2D random field of shear-wave velocity can be generated by developing a covariance function $C(h)$ between velocities at different locations via:

$$C(h) = \sigma^2_{\ln Vs} \rho(h) \qquad (4)$$

Four parameters are specified in the spatially correlated random field, namely, (1) the mean $\mu_{\ln Vs}$ and (2) standard deviation $\sigma_{\ln Vs}$ of shear-wave velocity in log scale for a lognormal distribution, (3) the horizontal correlation range R_{h,V_s}, and (4) the vertical correlation range R_{v,V_s} for specifying spatial correlations. Figure 1 shows realizations of V_s random fields with different horizontal/vertical correlation ranges. It can be observed in Fig. 1a that the V_s values follow a lognormal distribution with a relatively small correlation range (i.e. R_{h,V_s} and R_{v,V_s} = 6 m) in both horizontal and vertical directions. Figure 1b, c demonstrate a stronger horizontal spatial correlation with R_{h,V_s} = 100 m. Clearly, a larger correlation range corresponds to more uniformly distributed V_s field. Note that the correlation range in the horizontal direction is generally greater than that in the vertical
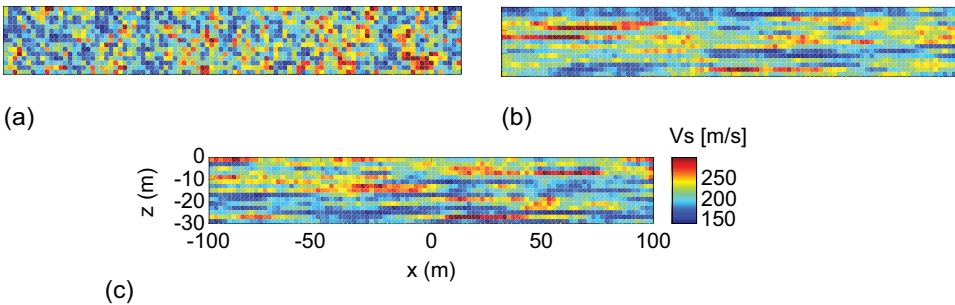

Figure 1. An illustrative example of spatially correlated shear-wave velocity random field, with the mean value of 200 m/s and $\sigma_{\ln Vs}$ = 0.2, (a) R_{h,V_s} = 6m, R_{v,V_s} = 6m ; (b) R_{h,V_s} = 100m, R_{v,V_s} = 6m ; (c) R_{h,V_s} = 100m, R_{v,V_s} = 2m.

direction, given that soils are often deposited horizontally layer by layer. It is also worth mentioning that the random field in Fig. 1 are just a small portion of a much bigger domain for illustration purpose, while entire domain in the numerical simulation is L = 2000 m in width and H = 30 m in thickness. We adopted V_s = 200 m/s as the mean value of shear-wave velocity and the damping ratio of 5% for all simulations throughout the study.

2.2. *Spectral Element Simulation (SEM)*

In this study, the SEM is adopted to simulate propagation of seismic waves in 2D heterogeneous soils using software package SPECFEM2D [Komatitsch and Vilotte, 1998]. The SEM is a high-order finite element method that uses a special nodal basis and pseudo-spectral method to achieve high accuracy in modeling wave propagation. The SEM method is superior to the commonly used finite-difference method in many ways. If a polynomial degree of 4 is used in interpolation, one SEM element per wavelength has been found to be sufficiently accurate [Wang *et al.*, 2017, 2018].

Throughout the study, the SEM mesh resolution is 2 m × 2 m in both horizontal and vertical directions, and the polynomial degree of 4 is used for interpolation, which is accurate for modeling wave propagation up to 100 Hz. The random velocity fields generated in the previous section are assigned to Gaussian points in SEM elements. An incident plane shear wave is input from the bottom displacement boundary. The upper boundary is a free surface and periodic condition is implemented on the left and right boundaries. A total of 1000 sampling stations are equally distributed on the surface of the computational domain. Only data in the middle 800 stations are used in the analyses throughout the study to eliminate any possible influence of boundary condition on the left and right ends.

2.3. *Validation of SEM Simulation Using a Uniform Ground*

In this study, the amplification factor $AF(f)$ is defined as the ratio of Fourier spectrum at the surface and at the base. A Ricker wavelet is used as acceleration input in the simulation, and uniform ground excitation is input at the base of the model, so the input motion is vertically propagated plane wave. The Ricker wavelet has been frequently used to model seismic input, and has been often used as a broad spectrum source in computational dynamics [Thompson *et al.*, 2009; Wang *et al.*, 2017, 2018]. Figure 2a,b shows an example of the Ricker wavelet and its frequency content. By choosing appropriate parameters, the wavelet contains sufficient intensity at the first four resonance frequencies of the site.

First, the 2D SEM simulation is validated by conducting a site response analysis for a uniform soil layer on a rigid base, where V_s = 200 m/s and H = 30 m. The amplification of ground motion can be defined by the ratio of motion at the ground surface (z = 0) and at the base (z = H). For an uniform damped soil on a rigid rock base, the amplification factor (or transfer function), $AF(f)$, depends on the frequency of motions, shear wave velocity of the soil and its thickness. The amplification factor can be theoretically determined by Eq. (5) [Kramer, 1996]:
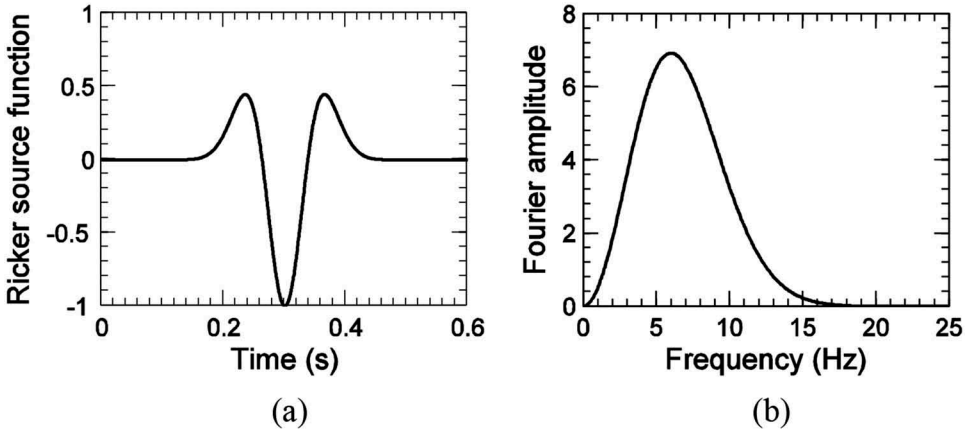
Figure 2. Time history and Fourier amplitude spectrum of the Ricker wavelet.

$$AF(f) = \left| \frac{u(t, z = 0)}{u(t, z = H)} \right| = \frac{1}{\left| \cos \frac{\omega H}{V_s(1+i\xi)} \right|} \approx \frac{1}{\sqrt{\left[\cos\left(\frac{\omega H}{V_s}\right) \right]^2 + \left(\frac{\xi \omega H}{V_s} \right)^2}} \tag{5}$$

where $u(t, z = 0)$ and $u(t, z = H)$ denote the displacement amplitude at the surface and at the base, $\omega = 2\pi f$ denotes wave angular frequency, H represents the soil thickness, V_s denotes shear wave velocity of the soil, ξ is the damping ratio.

Note Eq. (5) is applicable only for a uniform soil condition. The amplification factor $AF(f)$ is compared with the theoretical solution in Eq. (5). Figure 3a shows that the numerical results are almost identical to the theoretical solution ($\xi = 5\%$), where four resonance frequencies, denoted as f_1, f_2, f_3 and f_4, are also identified. As illustrated in Fig. 3b, the first resonance occurs when the frequency of input motion coincides with the natural frequency of soil column, which is 1.67 Hz in this case. Note that f_1, f_2, f_3 and f_4 correspond to a wavelength of 120, 40, 24 and 17 m, respectively.
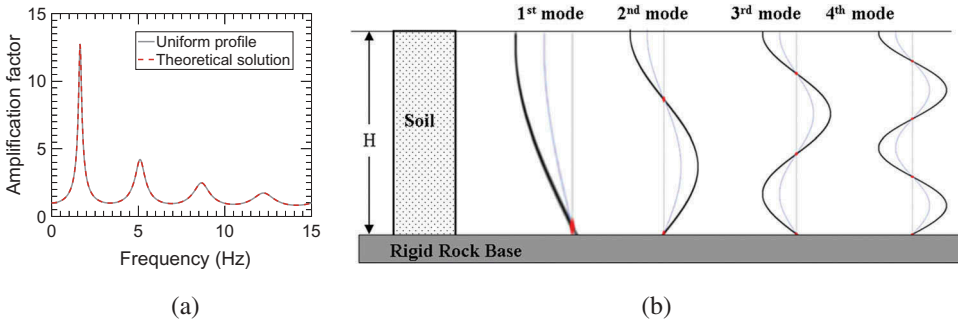

Figure 3. (a) Computed and theoretical amplification factor of a uniform ground ($\xi = 5\%$); (b) four fundamental modes of a standing wave in the soil.

3. Influence of Spatial Variability on Site Amplification

In this part, the effect of spatial variability in heterogeneous soils on 2D ground amplification is investigated by varying standard deviation and horizontal/vertical correlation ranges of V_s random fields. The shear-wave velocity follows a lognormal distribution with a mean of 200 m/s and standard deviations $\sigma_{\ln Vs}$ of 0.1, 0.2, 0.3 and 0.4 in the natural log scale. The horizontal correlation ranges (R_{h,V_s}) are assumed as 100 m, while the vertical ranges (R_{v,V_s}) are assumed as 6 m, respectively. 5% soil damping is used throughout the paper. Figure 4 shows realizations of amplification factors varying with the standard deviations $\sigma_{\ln Vs}$, where the first four resonance frequencies (f_1, f_2, f_3, f_4) of the uniform ground ($V_s = 200$m/s) are indicated by the dashed lines as the reference resonance frequencies. It is also worth noting that the amplifications at high resonance frequencies shift in the frequency domain with increasing $\sigma_{\ln Vs}$, which indicates that ground response of waves with a short wavelength (corresponding to high resonance frequency) is more influenced by the soil heterogeneity. In the meantime, spatial distribution of the amplification factor becomes highly variable with increasing soil heterogeneity, and the resonance frequencies even become not obvious at such cases.

Figure 5 shows the frequency-domain distribution of the amplification factors for the heterogeneous soil fields with different $\sigma_{\ln Vs}$. Note that the grey band represents distribution of the amplification factors at each monitoring point, with their mean value (in solid line)
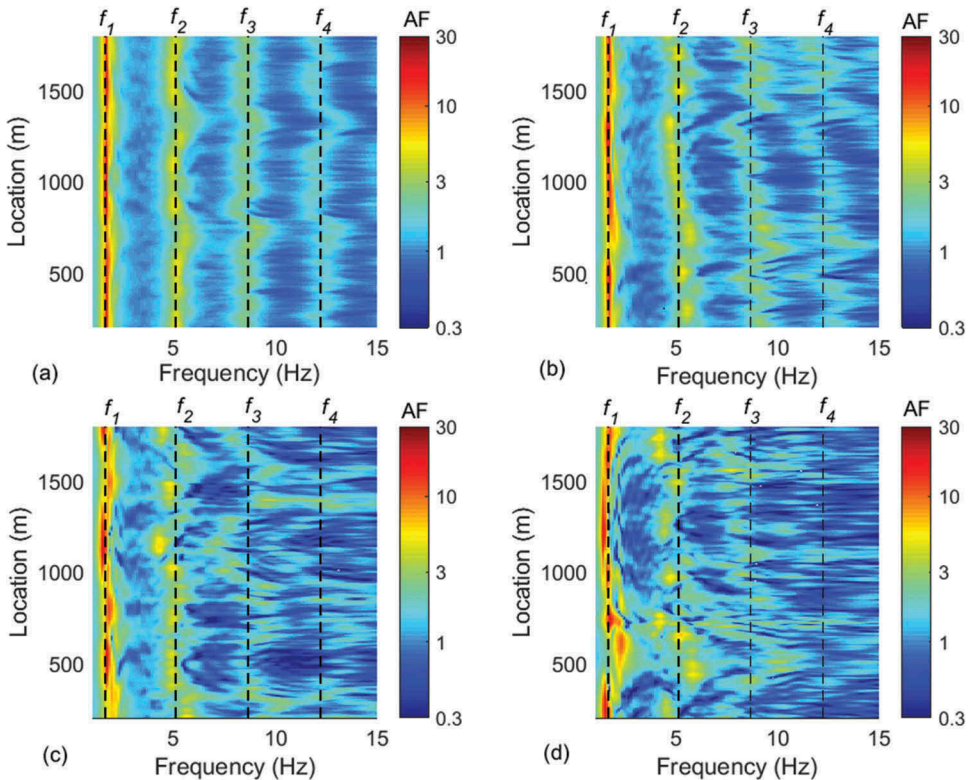

Figure 4. Spatial distribution of amplification factors for spatially correlated random fields with $R_{h,V_s} = 100$m, $R_{v,V_s} = 6$m, and (a) $\sigma_{\ln Vs} = 0.1$, (b) $\sigma_{\ln Vs} = 0.2$, (c) $\sigma_{\ln Vs} = 0.3$, (d) $\sigma_{\ln Vs} = 0.4$.

Figure 5. Variability of amplification factors for spatially correlated random fields with $R_{h,V_s} = 100m$, $R_{v,V_s} = 6m$, and (a) $\sigma_{\ln V_s} = 0.1$, (b) $\sigma_{\ln V_s} = 0.2$, (c)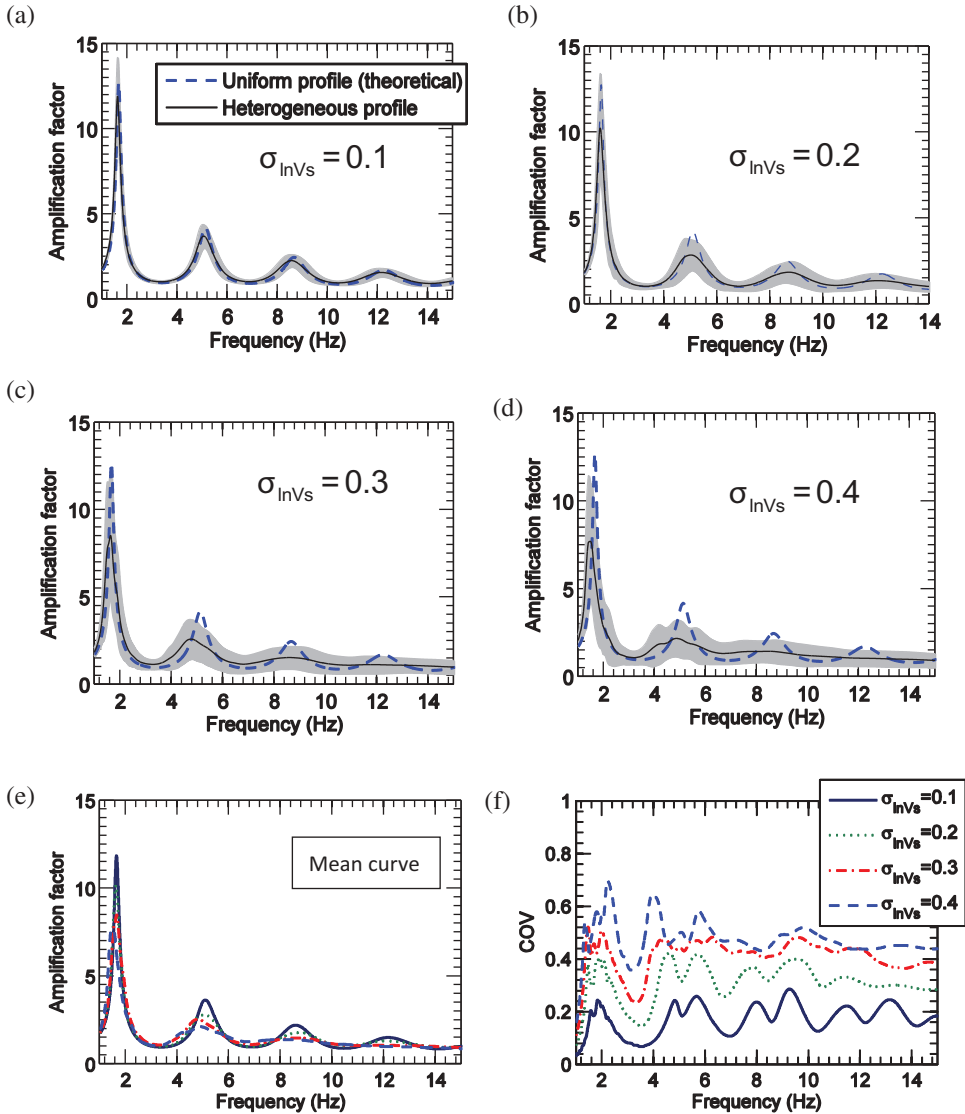 $\sigma_{\ln V_s} = 0.3$ and (d) $\sigma_{\ln V_s} = 0.4$ as well as (e) the mean curve and (f) coefficient of variation (COV) of the amplification factor in the frequency domain.

compared with the theoretical amplification of a uniform profile (in dashed line). When $\sigma_{\ln V_s}$ is relative small (0.1), ground amplifications in the heterogeneous soil yield similar results to that in the uniform soil profile, as demonstrated in Fig. 5a. Figure 5e shows that increase in $\sigma_{\ln V_s}$ reduces the mean amplification factors at the reference resonance frequencies due to wave scattering, reflection and deflection in the heterogeneous soil. Reduction in amplification seems to be more significant at high frequencies, because the wave length at high frequencies becomes comparable to the dimension of spatial variation. On the other hand, the influence of $\sigma_{\ln V_s}$ on coefficients of variations (COV) of amplification factors are

presented in Fig. 5f. For $\sigma_{\ln Vs} = 0.1$, the COV varies in the range of 0.1–0.2 with a larger COV of around 0.2 occurring at the resonance frequencies. As $\sigma_{\ln Vs}$ becomes larger, more scatter is observed in the amplification factors

As is demonstrated in Fig. 1, the spatial correlation of shear-wave velocity affects the distribution of V_s field. Therefore, it is important to investigate the seismic ground amplification for randomized V_s fields with different variations and spatial correlations. Figure 6 summarizes amplifications for all 16 cases with horizontal spatial correlation ranges $R_{h,V_s} = 6, 20, 50$ and 100 m, and standard deviations $\sigma_{\ln Vs} = 0.1, 0.2, 0.3$ and 0.4. First, when V_s fields have small variation (i.e. $\sigma_{\ln Vs} = 0.1$), sites for different spatial correlation ranges yield almost identical mean amplification factors, indicating that the influence of spatial correlation on ground response is marginal. Meanwhile, the COVs of ground amplification factors, as shown in the Fig. 6b, fall in the range of 0.05–0.2. On the other hand, when $\sigma_{\ln Vs}$ becomes larger, the effect of spatial correlation becomes more pronounced. For example, for the case $\sigma_{\ln Vs} = 0.4$, the COV of ground amplifications varies from 0.22 to 0.7 at the first resonance frequency, indicating that ground amplification is strongly influenced by horizontal correlation of the site. In general, the amplification is more scattered if R_{h,V_s} is larger. That is because for a smaller R_{h,V_s}, the soil profile is more "statistically" uniform, while a larger R_{h,V_s} corresponds to a more horizontally layered V_s field that is "statistically" nonuniform, as demonstrated in Fig. 1.

Figure 7 presents amplifications for 12 cases with $\sigma_{\ln Vs} = 0.1, 0.2, 0.3$ and 0.4, and the vertical spatial correlation ranges R_{v,V_s} equals 2, 6, 10 m. In general, increasing the vertical spatial correlation will increase the COV of ground amplification, but the effect is less significant as compared with the previous cases of horizontal spatial correlation. It can be also observed from Fig. 7a,c,e,g that the mean amplification curves are quite consistent for different vertical correlated V_s fields.

4. Spatial Correlation of Ground-motion Amplification

Distribution of spatial correlations of ground-motion amplification over the entire frequency range is studied in this section. Figure 8 illustrates the spatial distribution of amplification factors at the first four resonance frequencies with different horizontal correlation of shear wave velocity R_{h,V_s}.

Geostatistics analysis is performed to study the spatial correlation of the amplification factors. The semivariogram in the exponential form of Eq. (2) is used to fit the amplification factor distribution by a weighted least square method. Figure 9 illustrates the fitted semivariograms $\tilde{\gamma}(h)$ versus the separation distance h for an amplification frequency range of 0–15 Hz. By definition, the correlation range of the amplification factors, R_{AF}, can be determined as the separation distance where $\tilde{\gamma}(h)$ reaches 95% of its ultimate value. As shown in Figs. 9 and 10a,b, the contour line of R_{AF} is drawn over the amplification frequencies, representing propagation of spatial variability in the soil media to that in the ground amplification.

Figure 9 illustrates R_{AF} on a spatially correlated V_s field with $R_{h,V_s} = 20$ m and $R_{v,V_s} = 6$ m. Figure 10a,b illustrates R_{AF} on a spatially correlated V_s field with $R_{h,V_s} = 50$ m and $R_{v,V_s} = 6$ m. Figure 10c summarizes its relationship between R_{AF} and R_{h,V_s}. First, it can be observed that R_{AF} increases with R_{h,V_s} at all frequencies. R_{AF} around the 1st resonance frequencies (f_1) ranges from 160–260 m, and R_{AF} around the 2nd resonance frequencies (f_2) ranges from 60–200 m. They are all much larger than the specified R_{h,V_s} values. For R_{AF} at higher
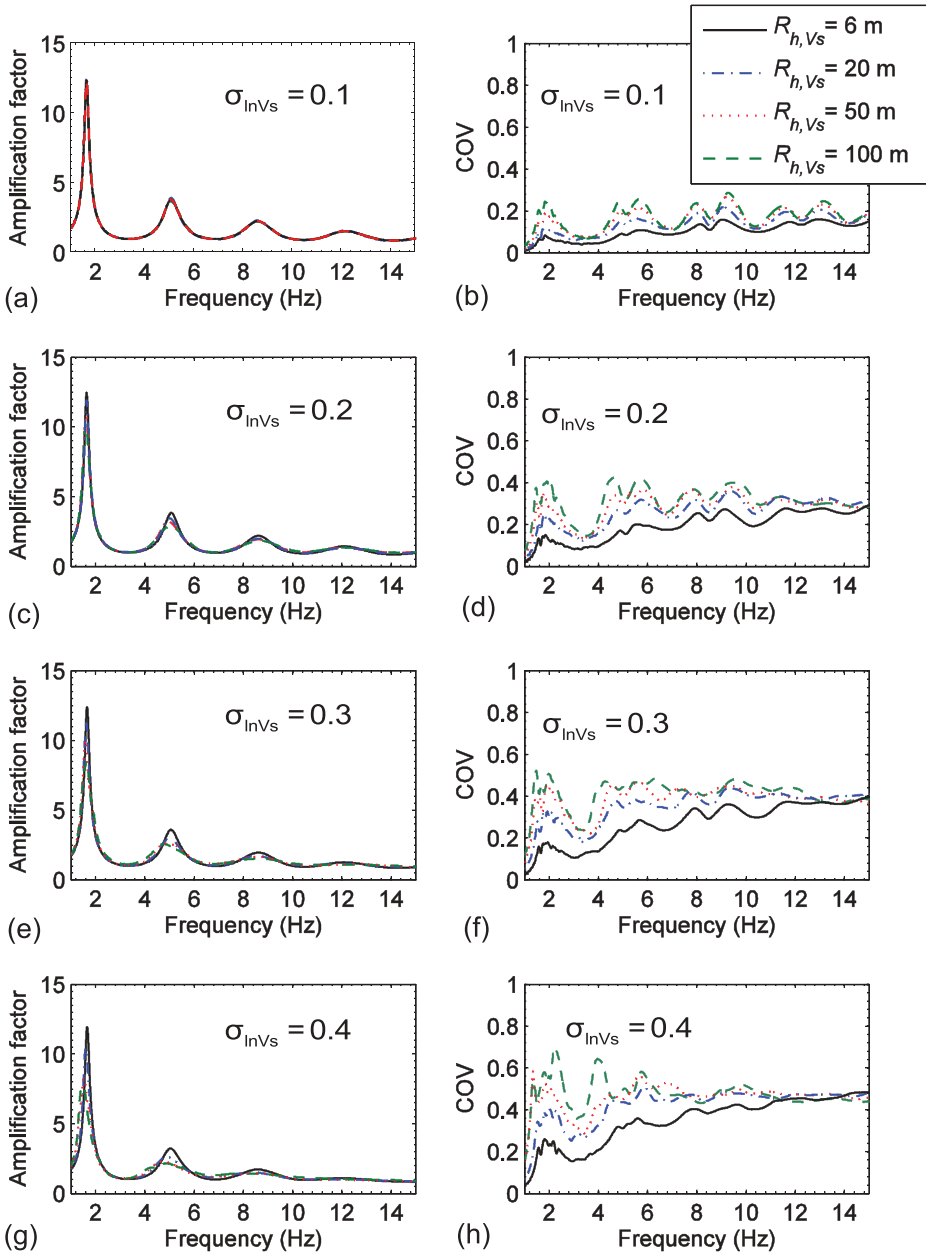
Figure 6. (a)(c)(e)(g) Mean and (b)(d)(f)(h) COVs of amplification factors for Vs fields with different horizontal correlations R_{h,V_s} and standard deviations $\sigma_{\ln Vs}$ ($R_{v,V_s} = 6m$ for all cases).

resonance frequencies (f_3, f_4), R_{AF} versus R_{h,V_s} data are in general around the 1:1 trend line, indicating that the spatial correlation of ground amplification at these high resonance frequencies approximately equals to the specified spatial correlation of the soil medium. For all cases, it also seems that the correlation range is not particularly affected by variation of V_s, when $\sigma_{\ln Vs}$ varies from 0.1, 0.2, 0.3 to 0.4.
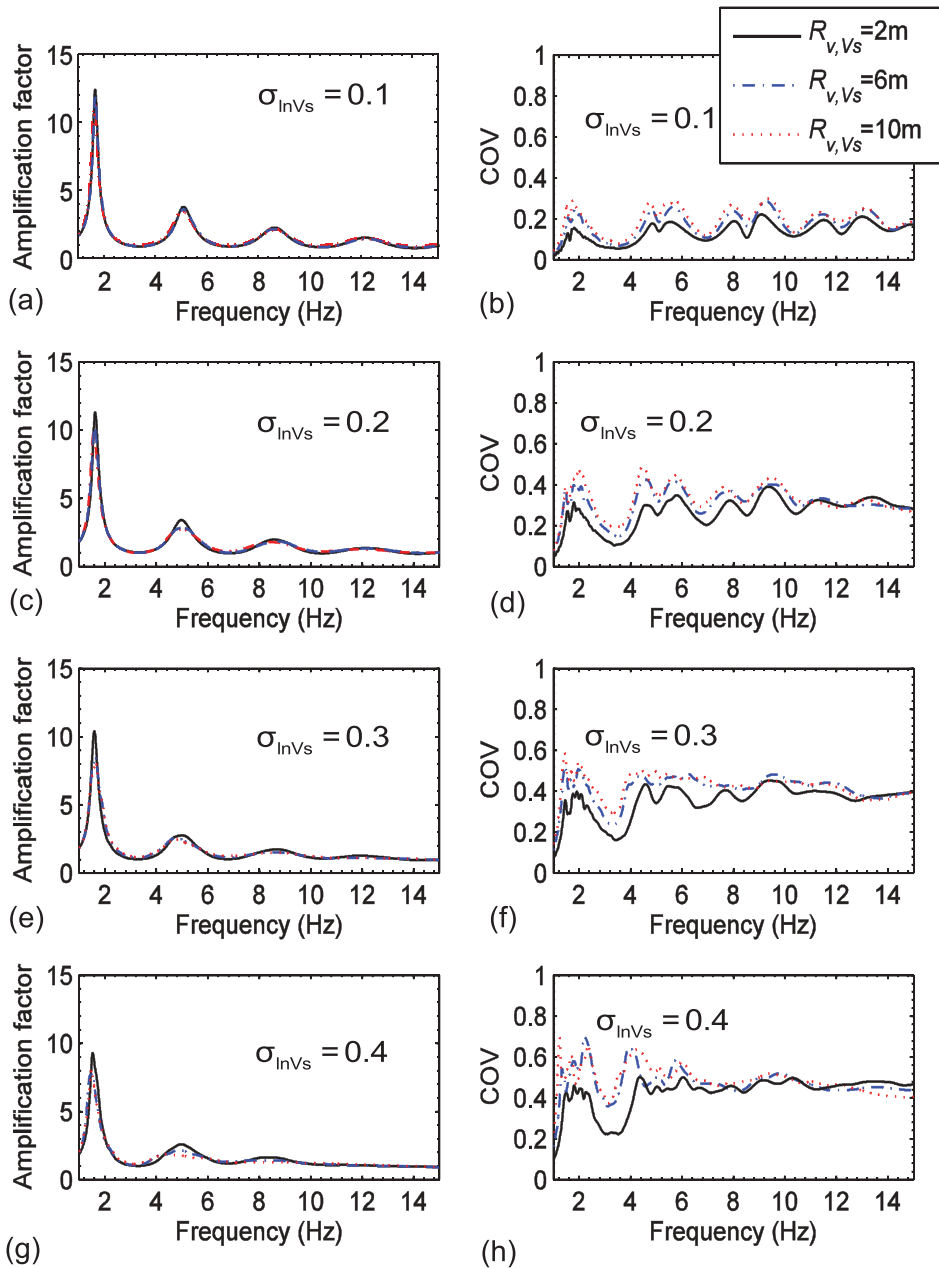
Figure 7. (a)(c)(e)(g) Mean and (b)(d)(f)(h) COVs of amplification factors for V_s fields with different vertical correlations R_{v,V_s} and standard deviations $\sigma_{\ln V_s}$ (R_{h,V_s} = 100m for all cases).

5. Conclusions

In this paper, extensive parametric studies have been conducted to quantify variability of the seismic amplification of viscoelastic ground with spatially varying shear wave velocity. The numerical simulation is based on 2D SEM, which adopts a pseudo-spectral approach
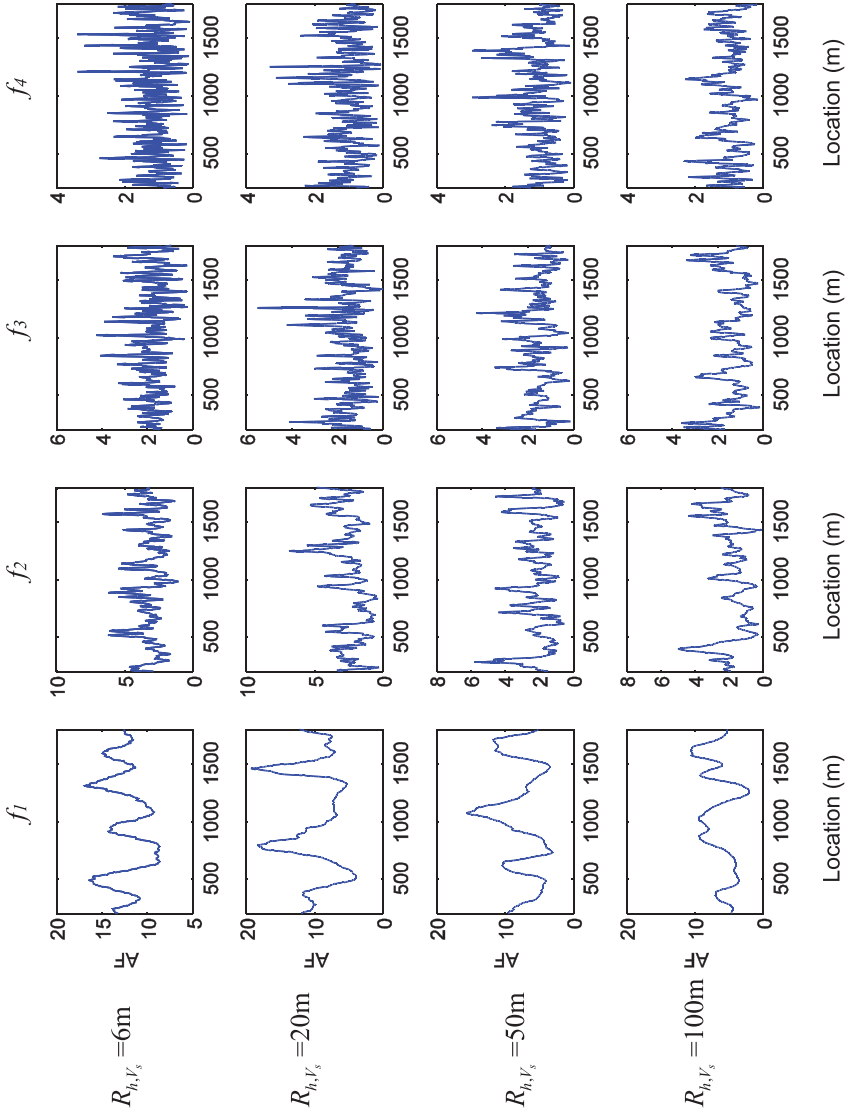
Figure 8. Spatial distribution of amplification factors at the first four resonance frequencies with different R_{h,V_s} (R_{v,V_s} = 6 m and $\sigma_{\ln V_s}$ = 0.2 for all cases).
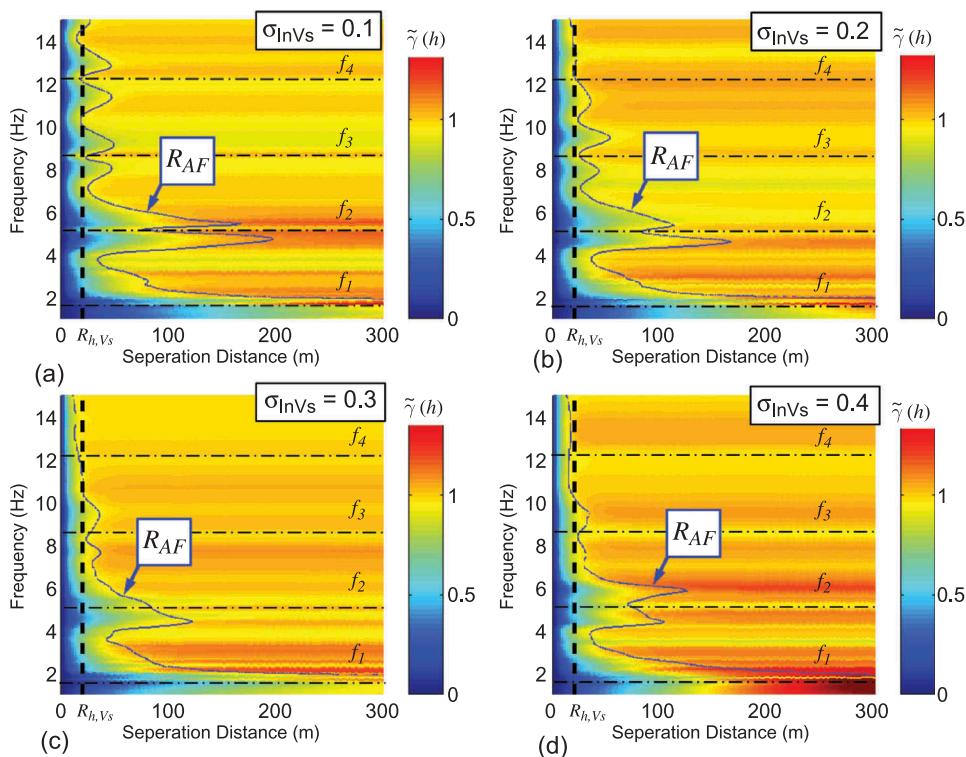
Figure 9. Semivariogram of the amplification factors over the frequency domain and contour lines for its horizontal correlation range R_{AF} (Note $R_{h,V_s} = 20$m, $R_{v,V_s} = 6$m for all cases, $\sigma_{\ln Vs} = 0.1, 0.2, 0.3, 0.4$).

to achieve high accuracy in modeling wave propagation. By varying the variance and spatial correlation of the shear wave velocity in both horizontal and vertical directions, soil sites with different levels of heterogeneity are modelled.

The 2D simulation results indicate that with increase in the standard deviation of shear wave velocity field, $\sigma_{\ln Vs}$, the peak values of the mean amplification factors at resonance frequencies are subdued due to wave scatter, reflection and deflection in the heterogeneous soil. Numerical simulations also demonstrate that COVs of amplification factors at resonance frequencies are slightly larger than the prescribed $\sigma_{\ln Vs}$ for the special case of $R_{h,V_s} = 100$ m, $R_{v,V_s} = 6$ m (Fig. 5). If R_{h,V_s} reduces to 50, 20 and 6 m, the site becomes less horizontally structured. The COVs of the amplification factors reduces significantly, particularly at the first three resonance frequencies (Fig. 6). On the other hand, reducing the spatial correlation of V_s in the vertical direction, R_{v,V_s}, from 10 to 2 m can also reduce the COVs of the amplification factors but in a less significant manner (Fig. 7). Note that the wavelengths corresponding to the first four resonance frequencies are 120, 40, 24 and 17 m, respectively. The analyses demonstrated that both of the length scales of the heterogeneity and the wave should be considered simultaneously when quantifying the variability of the seismic ground amplification.

Spatial correlations of ground-motion amplification over the entire frequency range are also investigated in this study. The spatial correlation ranges of ground amplification at the
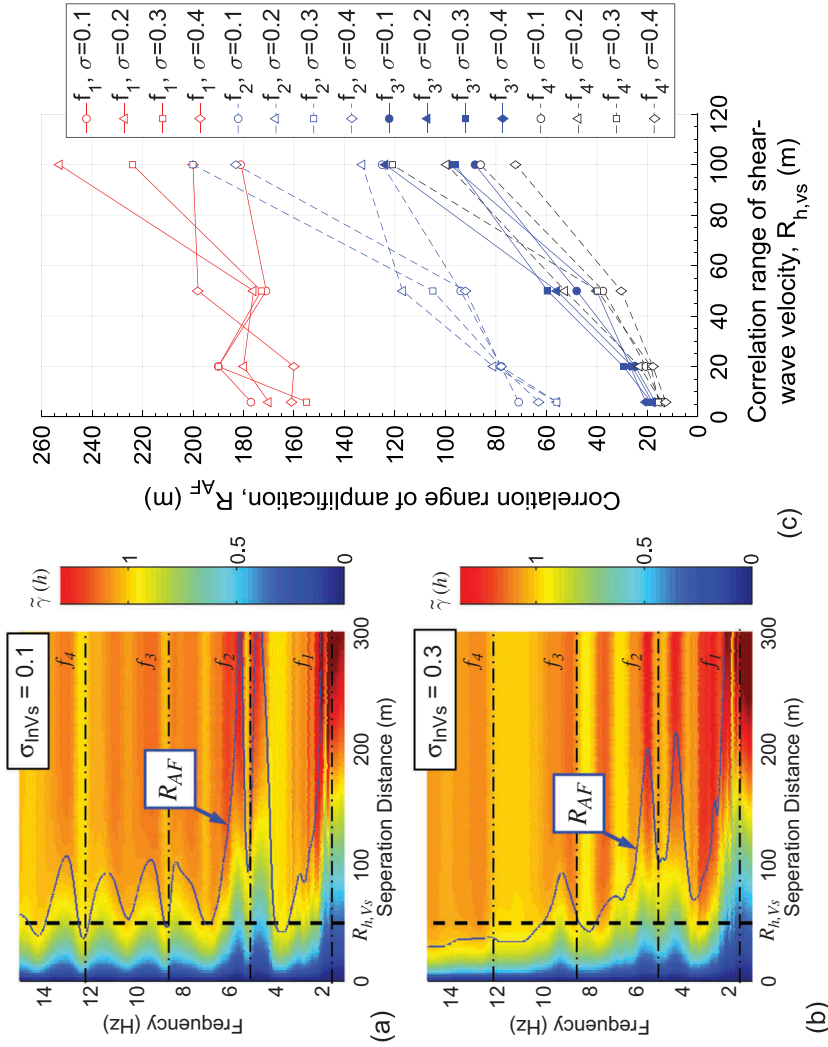
Figure 10. (a)(b) Semivariogram of the amplification factors over the frequency domain and contour line for its horizontal correlation range R_{AF} (Note R_{h,V_s} = 50m, R_{v,V_s} = 6m, $\sigma_{\ln V_s}$ = 0.1, 0.3), (c) Relations between correlation ranges of amplification and ranges of shear-wave velocity for resonance frequencies $f_1 - f_4$ and $\sigma_{\ln V_s}$ of 0.1, 0.2, 0.3 and 0.4 (R_{v,V_s} = 6m for all cases).

first two resonance frequencies (f_1, f_2) are substantially larger than the specified R_{h,V_s}, while the correlation ranges at high resonance frequencies (f_3, f_4) are similar to the prescribed R_{h,V_s}. Numerical results indicate that amplification of low frequency component (which is associated with a longer wavelength) would have a longer spatial correlation than that of the high frequency component, indicating the fact that propagation of variability on ground-motion amplification is frequency dependent. Yet, further research is still much needed to study the interplay of these various length scales, in order to improve scientific understanding of propagation of variability in seismic amplification of heterogeneous soils.

Funding

References

Afra, H. and Pecker, A. [2002] "Calculation of free field response spectrum of a non-homogeneous soil deposit from bed rock response spectrum," *Soil Dynamics and Earthquake Engineering* **22**(2), 157–165. doi:10.1016/S0267-7261(01)00056-2.

Bradley, B. A., Wotherspoon, L. M., Kaiser, A. E., Cox, B. R. and Jeong, S. [2018] "Influence of site effects on observed ground motions in the Wellington region from the Mw 7.8 Kaikoura, New Zealand, Earthquake," *Bulletin of Seismological Society of America* **108**(3), 1722–1735. doi:10.1785/0120170286.

DeGroot, D. J. [1996] "Analyzing spatial variability of in situ soil properties." *Proceedings of the 1996 conference on uncertainty in the geologic environment, Uncertainty'96.* Part I, 31 July-3 August, New York, USA: ASCE.

Du, W. and Wang, G. [2014] "Fully probabilistic seismic displacement analysis of spatially distributed slopes using spatially correlated vector intensity measures," *Earthquake Engineering & Structural Dynamics* **43**(5), 661–679. doi:10.1002/eqe.2365.

Elkateb, T., Chalaturnyk, R. and Robertson, P. K. [2003] "Simplified geostatistical analysis of earthquake-induced ground response at the wildlife site, California, USA," *Canadian Geotechnical Journal* **40**(1), 16–35. doi:10.1139/t02-089.

Flores-Estrella, H., Yussim, S. and Lomnitz, C. [2007] "Seismic response of the Mexico City Basin: A review of twenty years of research," *Natural Hazards* **40**(2), 357–372. doi:10.1007/s11069-006-0034-6.

Gazetas, G. [1982] "Vibrational characteristics of soil deposits with variable wave velocity," *International Journal for Numerical and Analytical Methods in Geomechanics* **6**, 1–20. doi:10.1002/(ISSN)1096-9853.

Goovaerts, P. [1997] *Geostatistics for Natural Resources*, Evaluation. Oxford University Press, Oxford, New York.

Hashash, Y. M. A. and Park, D. [2002] "Viscous damping formulation and high-frequency components in deep deposits," *Soil Dynamics and Earthquake Engineering* **22**(7), 611–624. doi:10.1016/S0267-7261(02)00042-8.

Holzer, T. L., Bennett, M. J., Noce, T. E. and Tinsley, J. C. [2005] "Shear-wave velocity of surficial geologic sediments in Northern California: statistical distributions and depth dependence," *Earthquake Spectra* **21**(1), 161–177. doi:10.1193/1.1852561.

Huang, D. and Wang, G. [2015a] "Stochastic simulation of regionalized ground motions using wavelet packets and cokriging analysis," *Earthquake Engineering & Structural Dynamics* **44**, 775–794. doi:10.1002/eqe.2487.

Huang, D. and Wang, G. [2015b] "Region-specific spatial cross-correlation model for stochastic simulation of regionalized ground-motion time histories," *Bulletin of Seismological Society of America* **105**(1), 272–284. doi:10.1785/0120140198.

Huang, D., Wang, G., Wang, C. and Jin, F. [2018] "A modified frequency-dependent equivalent linear method for seismic site response analyses and model validation using KiK-net borehole arrays," *Journal of Earthquake Engineering* published online. DOI: 10.1080/13632469.2018.1453418.

Idriss, I. and Sun, J. I. [1992] "SHAKE91: A computer program for conducting equivalent linear seismic response analyses of horizontally layered soil deposits. Center for Geotechnical Modelling," Department of Civil and Environmental Engineering, University of California, Davis

Kaklamanos, J., Baise, L. G., Thompson, E. M. and Dorfmann, L. [2015] "Comparison of 1D linear, equivalent-linear, and nonlinear site response models at six KiK-net validation sites," *Soil Dynamics and Earthquake Engineering* **69**, 207–219. doi:10.1016/j.soildyn.2014.10.016.

Kaklamanos, J., Bradley, B. A., Thompson, E. M. and Baise, L. G. [2013] "Critical parameters affecting bias and variability in site-response analyses using KiK-net downhole array data," *Bulletin of Seismological Society of America* **103**(3), 1733–1749. doi:10.1785/0120120166.

Kawase, H. [1996] "The cause of the damage belt in Kobe: The Basin-Edge Effect, constructive interference of the direct S-wave with the basin-Induced diffracted/Rayleigh waves," *Seismological Research Letter* **67**(5), 25–34. doi:10.1785/gssrl.67.5.25.

Komatitsch, D. and Vilotte, J. P. [1998] "The spectral element method: an efficient tool to simulate the seismic response of 2D and 3D geological structures," *Bulletin of Seismological Society of America* **88**(2), 368–392.

Kramer, S. L. [1996] *Geotechnical Earthquake Engineering*, Prentice Hall, New Jersey.

Mylonakis, G. E., Rovithis, E. and Parashakis, H. [2011] "1D seismic response of soil: continuously inhomogeneous vs equivalent homogeneous soil", III ECCOMAS Thematic Conference on Computational Methods in Structural Dynamics and Earthquake Engineering, M. Papadrakakis, M. Fragiadakis and V. Plevris (eds.) Corfu, Greece, 25–28 May 2011

Park, D. and Hashash, Y. M. A. [2004] "Soil damping formulation in nonlinear time domain site response analysis," *Journal of Earthquake Engineering* **8**(2), 249–274. doi:10.1080/13632460409350489.

Pehlivan, M., Rathje, E. M. and Gilbert, R. B. [2012] "Influence of 1D and 2D spatial variability on site response analysis," The 15th World Conference on Earthquake Engineering, September 24 to September 28, 2012, Lisbon, Portugal doi:10.1094/PDIS-11-11-0999-PDN

Rathje, E. M., Kotte, A. R. and Trent, W. L. [2010] "Influence of input motion and site property variabilities on seismic site response analysis," *Journal of Geotechnical and Geoenvironmental Engineering* **136**(4), 607–619. doi:10.1061/(ASCE)GT.1943-5606.0000255.

Rovithis, E. N., Parashakis, H. and Mylonakis, G. E. [2011] "1D harmonic response of layered inhomogeneous soil: Analytical investigation," *Soil Dynamics and Earthquake Engineering* **31**(7), 879–890. doi:10.1016/j.soildyn.2011.01.007.

Schnabel, P., Lysmer, J. and Seed, H. [1972] "SHAKE-A computer program for response analysis of horizontally layered sites," Report No. EERC 72-12, University of California at Berkeley.

Soulie, M., Montes, P. and Silvestri, V. [1990] "Modeling spatial variability of soil parameters," *Canadian Geotechnical Journal* **27**(5), 617–630. doi:10.1139/t90-076.

Thompson, E. M., Baise, L. G., Kayen, R. E. and Guzina, B. B. [2009] "Impediments to predicting site response: seismic property estimation and modeling simplifications," *Bulletin of Seismological Society of America* **99**, 2927–2949. doi:10.1785/0120080224.

Thompson, E. M., Baise, L. G., Tanaka, Y. and Kayen, R. E. [2010] "A taxonomy of site response complexity," *Soil Dynamics and Earthquake Engineering* **41**, 32–43. doi:10.1016/j.soildyn.2012.04.005.

Towhata, I. [1996] "Seismic wave propagation in elastic soil with continuous variation of shear modulus in the vertical direction," *Soils and Foundations* **36**(1), 61–72. doi:10.3208/sandf.36.61.

Travasarou, T. and Gazetas, G. [2004] "On the linear seismic response of soils with modulus varying as a power of depth - The Maliakos marine clay," *Soils and Foundations* **44**(5), 85–93. doi:10.3208/sandf.44.5_85.

Wang, G., Du, C. and Huang, D. [2017] "Large-scale simulation of ground motion amplification considering 3D topography and subsurface soil condition," PBD III, Vancouver, July 2017

Wang, G., Du, C., Huang, D., Jin, F., Koo, R. C. H. and Kwan, J. S. H. [2018] "Parametric models for 3D topographic amplification of ground motions considering subsurface soils," *Soil Dynamics and Earthquake Engineering* **115**, 41–54. doi:10.1016/j.soildyn.2018.07.018.

Wang, G. and Du, W. [2013] "Spatial cross-correlation models for vector intensity measures (PGA, Ia, PGV, and SAs) considering regional site conditions," *Bulletin of Seismological Society of America* **103**(6), 3189–3204. doi:10.1785/0120130061.

Wu, Y., Zhou, X., Gao, Y., Zhang, L. and Yang, J. [2019] "Effect of soil variability on bearing capacity accounting for non-stationary characteristics of undrained shear strength," *Computers and Geotechnics* **110**, 199–210. doi:10.1016/j.compgeo.2019.02.003.

Zhang, N., Gao, Y. and Pak, R. Y. S. [2017] "Soil and topographic effects on ground motion of a surficially inhomogeneous semi-cylindrical canyon under oblique incident SH waves," *Soil Dynamics and Earthquake Engineering* **95**, 17–28. doi:10.1016/j.soildyn.2017.01.037.

Zhang, N., Zhang, Y., Gao, Y., Pak, R. Y. S., Wu, Y. and Zhang, F. [2019] "An exact solution for SH-wave scattering by a radially multi-layered inhomogeneous semi-cylindrical canyon," *Geotechnical Journal International* **217**(2), 1232–1260.